International Journal of Electrical, Electronic and Communication Sciences
ISSN: 2517-9438
Vol:5, No:12, 2011

Averaging Model of a Three-Phase Controlled Rectifier Feeding an Uncontrolled Buck Converter

P. Ruttanee, K-N. Areerak*, and K-L. Areerak

Abstract**—**Dynamic models of power converters are normally time-varying because of their switching actions. Several approaches are applied to analyze the power converters to achieve the time-invariant models suitable for system analysis and design via the classical control theory. The paper presents how to derive dynamic models of the power system consisting of a three-phase controlled rectifier feeding an uncontrolled buck converter by using the combination between the well known techniques called the DQ and the generalized state-space averaging methods. The intensive time-domain simulations of the exact topology model are used to support the accuracies of the reported model. The results show that the proposed model can provide good accuracies in both transient and steady-state responses.

Keywords**—**DQ method, Generalized state-space averaging method, Three-phase controlled rectifier, Uncontrolled buck converter, Averaging model, Modeling, Simulation.

I. Introduction

POWER converters are widely used in many applications. The dynamic model of the system including the power electronic converter is very important for system design and analysis. It is well known that the power converter models are time-varying because of their switching behavior. Several approaches are commonly used for eliminating the switching actions to achieve time-invariant model based on averaging models. Then, the classical linear control theory can be easily applied to the model for a system analysis and design.

The first method is the generalized state-space averaging (GSSA) modeling method. This method has been used to analyze many power converters in DC distribution systems [1], as well as uncontrolled and controlled rectifiers in single-phase AC distribution systems [2] and 6- and 12- pulse diode rectifiers in three phase systems [3]. The second is an average-value (AV) modeling method, which has been used for 6- and 12- pulse diode rectifiers in many publications [4], as well as generators with line-commutated rectifiers [5]. These rectifiers can be modeled with good accuracy as a constant DC voltage source. However, this method is not easily applicable to analyze the general AC power system with multi-converter power electronic systems. Another technique widely used for AC system analysis is that of DQ-transformation theory [6-8], in which power converters can be treated as transformers. The resulting converter models can be easily combined with models of other power elements expressed in terms of synchronously rotating frames such as generators, front-end converters, and vector-controlled drives. The DQ models of three-phase AC-DC power systems have been reported in the previous works for stability studies of the power system including a constant power load (CPL) [9]-[11]. The DQ method for modeling the three-phase uncontrolled and controlled rectifier has been reported in [9] and [12], respectively.

From the literature reviews, this paper presents the combination between the DQ modeling approach and the GSSA modeling method to derive the dynamic model of a controlled three-phase rectifier feeding an uncontrolled buck converter. According to the advantages of DQ and GSSA methods, the DQ method is selected to analyze the controlled three-phase rectifier including the transmission line components on AC side, while the GSSA method is used to analyze the buck converter. The proposed model is validated by the intensive time-domain simulation via the exact topology model of the commercial software package. The results show that the proposed mathematical models provide high accuracies in both transient and steady-state responses. Hence, the reported model is suitable for the system analysis and design via the classical control theory.

The paper is structured as follows. The power system considered is explained in Section II. In Section III, deriving the dynamic model of a controlled three-phase rectifier feeding a buck converter using the combination between DQ and GSSA methods is fully described. In Section IV, the model validation using the intensive-time domain simulation of the exact topology model is illustrated. Finally, Section V concludes and discusses the advantages of the DQ and GSSA modeling methods to derive the model of the power electronic system.

II. Power System Definition and Assumptions

The studied power system in the paper is depicted in Fig. 1. It consists of a balanced three-phase voltage source, transmission line represented by R_{eq}, L_{eq}, and C_{eq}, three-phase

P.Ruttanee, master student in electrical engineering, PEMC research group, School of Electrical Engineering, Suranaree University of Technology Nakhon Ratchasima, 30000, THAILAND.

*K-N. Areerak, lecturer, PEMC research group, School of Electrical Engineering, Suranaree University of Technology, Nakhon Ratchasima, 30000, THAILAND (corresponding author: kongpan@sut.ac.th)

K-L. Areerak, lecturer, PEMC research group, School of Electrical Engineering, Suranaree University of Technology, Nakhon Ratchasima, 30000, THAILAND.

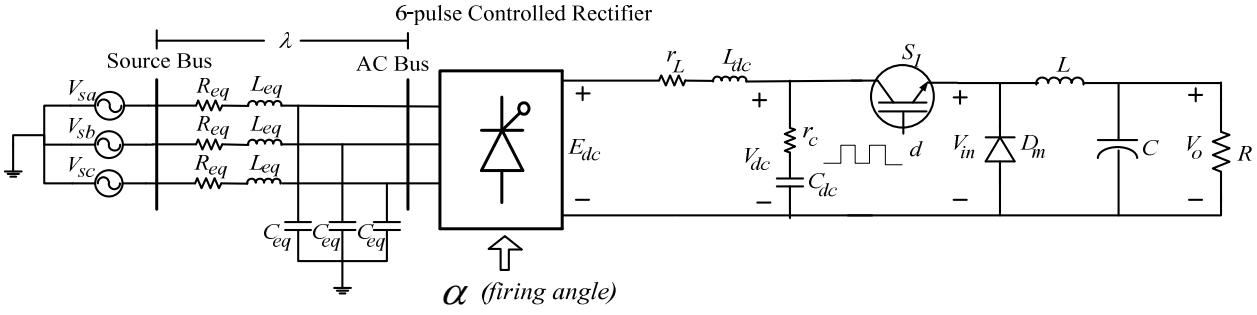

Fig. 1 The considered power system

controlled rectifier, and DC-link filters shown by elements r_L, L_{dc}, r_c (ESR) and C_{dc} feeding an uncontrolled buck converter. It is assumed that the controlled rectifier and the buck converter are operated under a continuous conduction mode (CCM) and the higher harmonics of the fundamental are neglected. E_{dc} and V_{dc} are the output terminal voltage of a controlled rectifier and the voltage across the DC-link capacitor C_{dc}, respectively. A phase shift between the source bus and the AC bus is λ as shown in Fig. 1.

The set of system parameters for the power system of Fig. 1 is given in Table I.

TABLE I
PARAMETERS OF THE SYSTEM IN FIG. 1

Parameter	Value
V_s	220 $V_{rms/phase}$
ω	2πx50 rad/s
R_{eq}	0.1 Ω
L_{eq}	24 μH
C_{eq}	2 nF
r_L	0.01 Ω
r_c	0.01 Ω
L_{dc} ($\Delta I_{dc} \leq$ 1.5 A)	50 mH
C_{dc} ($\Delta V_{dc} \leq$ 50 V)	500 μF
L ($\Delta I_L \leq$ 0.5 A)	14.168 mH
C ($\Delta V_o \leq$ 50 mV)	125 μF
R	20 Ω

III. DERIVING DYNAMIC MODELS

In the paper, the DQ method is used to analyze the three-phase controlled rectifier, while the GSSA approach is applied to eliminate the switching action of the buck converter. The details how to derive the dynamic model of the considered system in Fig.1 are fully explained in this section.

A. DQ method

The DQ modeling method is selected to derive the dynamic model of a three-phase controlled rectifier in which such rectifier can be treated as a transformer. According to Fig. 1, The effect of L_{eq} on the AC side causes an overlap angle μ in the output waveforms that causes as a commutation voltage drop. This drop can be represented as a variable resistance r_μ that is located on the DC side [13] as shown in Fig. 2. The r_μ can be calculated by:

$$r_\mu = \frac{3\omega L_{eq}}{\pi} \tag{1}$$

where ω is the source frequency.

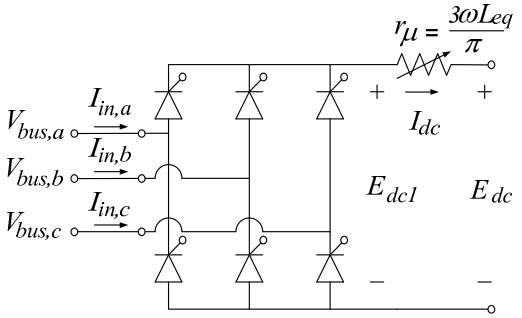

Fig. 2 Three-phase controlled rectifier with the overlap angle resistance

It can be seen from Fig. 2 that E_{dc1} represents the output voltage from the switching signal without an overlap angle effect, while E_{dc} represents the voltage at the rectifier output terminal taking onto account the voltage drop effect. Since the commutation effect has been moved on to the DC side, the switching signals for three-phase controlled rectifier can be applied without considering the effect of overlap angle. This is show in Fig. 3 in which α is the firing angle of thyristors.

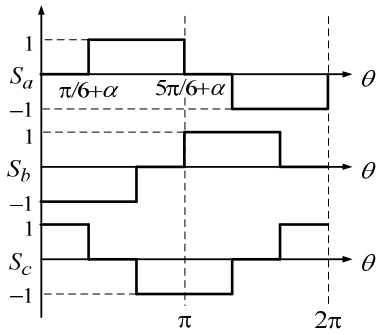

Fig. 3 The switching functions of three-phase controlled rectifier

The switching function of S_a in Fig. 3 can be expressed by a Fourier series. In this paper, neglecting the harmonics of the power system, the switching functions can be written for three phases as:

$$\mathbf{S_{abc}}=\frac{2\sqrt{3}}{\pi}\left[\sin(\omega t+\varphi-\alpha)\ \sin(\omega t-\frac{2\pi}{3}+\varphi-\alpha)\ \sin(\omega\ t+\frac{2\pi}{3}+\varphi-\alpha)\right]^{\mathrm{T}} \quad (2)$$

where ϕ is a phase angle of the AC bus voltage and α is the firing angle.

The relationship between input and output terminal of controlled rectifier is given by:

$$\mathbf{I_{in,abc}} = \mathbf{S_{abc}} I_{dc} \quad (3)$$

$$E_{dc1} = \mathbf{S_{abc}^{T}} \mathbf{V_{bus,abc}} \quad (4)$$

It can be seen from (3) that the fundamental input current is in phase with the switching signals. In addition, for a controlled rectifier, the fundamental input current lags the fundamental input voltage by α [13]. Equations (2)-(4) will be used to derive the model of controlled rectifier by using DQ modeling method as follows:

Firstly, the controlled rectifier is transformed into a two axis frame (DQ frame) rotating at the system frequency ω by means of:

$$\mathbf{T}[\theta(t)]=\sqrt{\frac{2}{3}}\begin{bmatrix}\cos(\theta(t)) & \cos(\theta(t)-\frac{2\pi}{3}) & \cos(\theta(t)+\frac{2\pi}{3})\\ -\sin(\theta(t)) & -\sin(\theta(t)-\frac{2\pi}{3}) & -\sin(\theta(t)+\frac{2\pi}{3})\end{bmatrix} \quad (5)$$

where $\theta(t) = \omega t - \frac{\pi}{2} + \phi_1$

Combining equations (3)-(5) results in:

$$\mathbf{I_{in,dq}} = \mathbf{S_{dq}} I_{dc} \quad (6)$$

$$E_{dc1} = \mathbf{S_{dq}^{T}} \mathbf{V_{bus,dq}} \quad (7)$$

Secondly, the switching functions in (2) can be transformed into a DQ frame by means of (5) to give:

$$\mathbf{S_{dq}}=\sqrt{\frac{3}{2}}\cdot\frac{2\sqrt{3}}{\pi}\left[\cos(\phi_1-\phi+\alpha)\quad -\sin(\phi_1-\phi+\alpha)\right]^{T} \quad (8)$$

The vector diagram for the DQ transformation is as shown in Figure 4 where V_s is the peak amplitude phase voltage, I_{in} is the peak amplitude current, V_{bus} is the peak amplitude AC bus voltage, and S is peak amplitude of the switching signal, here equal to $2\sqrt{3}/\pi$ as shown in (2).

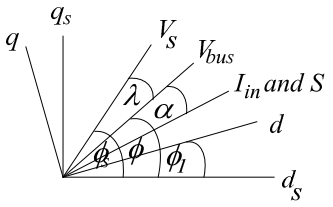

Fig. 4 The vector diagram for the DQ method

From (6)-(8), the controlled rectifier can be easily represented as a transformer having d and q-axis transformer ratio S_d, S_q that depend on the phase of the DQ frame (ϕ_1), the phase of V_{bus} (ϕ), and the firing angle of thyristors (α). As a result, the equivalent circuit of the controlled rectifier in the DQ frame derived by using DQ modeling method is shown in Fig. 5.

.

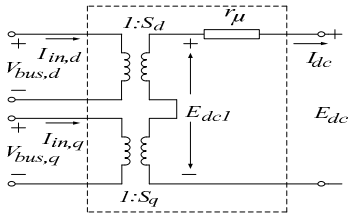

Fig. 5 The equivalent circuit of controlled rectifier on DQ frame

Finally, using (5), the cable section can be transformed into DQ frame [14]. The DQ representation of the cable is then combined with the controlled rectifier as shown in Fig. 5. As a result, the equivalent circuit of the power system in Fig.1 can be represented in the DQ frame as depicted in Fig. 6.The equivalent circuit in Fig. 6 can be simplified by fixing the rotating frame on the phase of the switching function ($\phi_1 = \phi - \alpha$). This results in the circuit as shown in Fig. 7.In Fig. 7, the three-phase controlled rectifier including the transmission line on AC side is transformed into the DQ frame via the DQ modeling method. Notice that the controlled rectifier can be modeled as the transformer in which it can provide the time-invariant model. The GSSA modeling method is then used to eliminate the switching action of the uncontrolled buck converter. The details how to derive the dynamic model of the power system as shown in Fig. 7 by using the GSSA method are given in Section B.

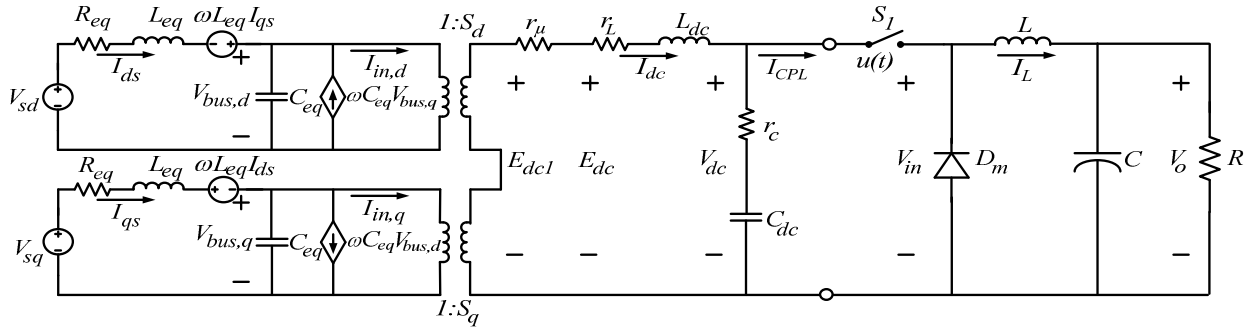

Fig. 6 The equivalent circuit of the power system in Fig. 1 on DQ frame

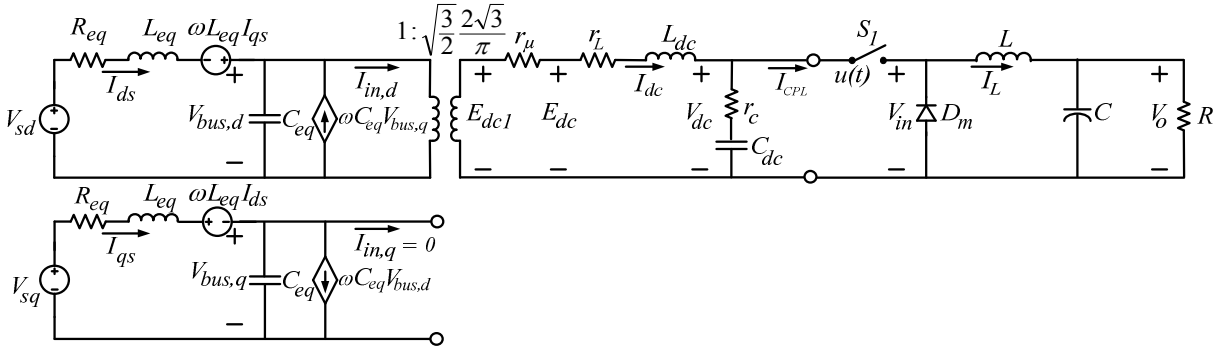

Fig. 7 The simplified equivalent circuit of the power system

B. GSSA method

The GSSA method is an alternative method to eliminate the time-varying switching function to achieve a time-invariant power converter model. The approach uses the time-dependent coefficients of the complex Fourier series as the state variables. The overview of this approach is as follows.

In general, a periodic waveform with period T can be represented by the complex Fourier series of the form

$$f(t) = \sum_{k=-\infty}^{\infty} \langle x \rangle_k (t) e^{jk\omega_s t} \tag{9}$$

where $\omega_s = 2\pi/T$ and $\langle x \rangle_k (t)$ is the complex Fourier coefficients.

The GSSA approach uses the $\langle x \rangle_k (t)$ of the waveform as the state variables of the system. These coefficients can be determined by

$$\langle x \rangle_k (t) = \frac{1}{T} \int_{t-T}^{t} f(t) e^{-jk\omega_s t} dt \tag{10}$$

The necessary properties of the $\langle x \rangle_k (t)$ for modeling the power system using the GSSA technique are as follows:

- differentiation with respect to time:

$$\frac{d\langle x \rangle_k}{dt} = \left\langle \frac{dx}{dt} \right\rangle_k - jk\omega_s \langle x \rangle_k \tag{11}$$

- the convolution relationship:

$$\langle xy \rangle_k = \sum_i \langle x \rangle_{k-i} \langle y \rangle_i \tag{12}$$

- if $f(t)$ is real (real-value periodic waveform),

$$\langle x \rangle_{-k} = \overline{\langle x \rangle_k} = \langle x \rangle_k^* \tag{13}$$

In (9) and (10), the value of k depends on the accuracy level. Theoretically, if k approaches infinity, the approximation error approaches zero. If the waveform can be assumed to have no ripple, it can be set to $k = 0$ called zero-order approximation [1]. On the other hand, if the waveform is similar to a sinusoidal signal, k can normally be set to -1, 1. This particular case is referred to as the first harmonic approximation [2].

For deriving the dynamic model of a buck converter using GSSA method, the switching function of such converter under the continuous conduction mode (CCM) is firstly defined in (14).

$$u(t)=\begin{cases} 1, & 0<t<dT_s \\ 0, & dT_s<t<T_s \end{cases} \tag{14}$$

where d is the duty cycle of the switch S_1 as shown in Fig. 7.

For the buck converter of Fig. 7, when the switch S_1 is closed, $I_{CPL} = I_L$ and $V_{dc} = V_{in}$. Otherwise, when the switch S_1 is opened, $I_{CPL} = 0$ and $V_{in} = 0$ by assuming no voltage drop acrossing diode D_m. Hence, the relationship between I_{CPL} and I_L, and the relationship between V_{dc} and V_{in} in terms of $u(t)$ are given by:

$$\begin{cases} I_{CPL} = u(t) I_L \\ V_{in} = u(t) V_{dc} \end{cases} \tag{15}$$

Applying the KVL and KCL to Fig. 7 with (14) and (15), the set of time-varying differential equations are given by:

$$\begin{cases} \dot{I}_{sd} = -\frac{R_{eq}}{L_{eq}} I_{sd} + \omega I_{sq} - \frac{1}{L_{eq}} V_{bus,d} + \frac{1}{L_{eq}} \sqrt{\frac{3}{2}} V_m \cos(\lambda+\alpha) \\ \dot{I}_{sq} = -\omega I_{sd} - \frac{R_{eq}}{L_{eq}} I_{sq} - \frac{1}{L_{eq}} V_{busq} + \frac{1}{L_{eq}} \sqrt{\frac{3}{2}} V_m \sin(\lambda+\alpha) \\ \dot{V}_{busd} = \frac{1}{C_{eq}} I_{sd} + \omega V_{busq} - \sqrt{\frac{3}{2}} \cdot \frac{2\sqrt{3}}{\pi C_{eq}} I_{dc} \\ \dot{V}_{busq} = -\omega V_{busd} + \frac{1}{C_{eq}} I_{sq} \\ \dot{I}_{dc} = \sqrt{\frac{3}{2}} \cdot \frac{2\sqrt{3}}{\pi L_F} V_{busd} - \left(\frac{r_\mu}{L_{dc}} + \frac{r_L}{L_{dc}} + \frac{r_c}{L_{dc}} \right) I_{dc} - \frac{1}{L_{dc}} V_{dc} + \frac{r_C \cdot u(t)}{L_{dc}} I_L \\ \dot{V}_{dc} = \frac{1}{C_{dc}} I_{dc} - \frac{u(t)}{C_{dc}} I_L \\ \dot{I}_L = \frac{u(t)}{L} V_{dc} - \frac{1}{L} V_o \\ \dot{V}_o = \frac{1}{C} I_L - \frac{1}{RC} V_o \end{cases} \tag{16}$$

As mentioned before, the switching behavior of the three-phase rectifier was eliminated by the DQ modeling approach. However, the time varying function, here is $u(t)$ in (16), still occur in the model due to the switch of a buck converter. Therefore, in the paper the GSSA method is used for eliminating the switching action of the buck converter to achieve the time-invariant model. The state-variables of the model are the Fourier coefficients of I_{sd}, I_{sq}, $V_{bus,d}$, $V_{bus,q}$, I_{dc}, V_{dc}, I_L, and V_o. Using the zero-order approximation by neglecting ripples on the DC waveforms, we can define 8 state variables:

$$\begin{cases} \langle I_{sd} \rangle_0 = I_{sd} \\ \langle I_{sq} \rangle_0 = I_{sq} \\ \langle V_{sd} \rangle_0 = V_{sd} \\ \langle V_{sq} \rangle_0 = V_{sq} \\ \langle I_{dc} \rangle_0 = I_{dc} \\ \langle V_{dc} \rangle_0 = V_{dc} \\ \langle I_L \rangle_0 = I_L \\ \langle V_o \rangle_0 = V_o \end{cases} \tag{17}$$

Using (10) to obtain the complex Fourier coefficient of the switching function in (14), the coefficient for the zero-order approximation can be determined as:

$$\langle u \rangle_0 = d \tag{18}$$

where d is the duty cycle of the buck converter.

Then, applying (11)-(13) to (16) and substituting the Fourier coefficient of the switching signal as given in (18), the dynamic model of the system in Fig. 7 using GSSA modeling method can be expressed in (19).

$$\begin{cases} \dot{I}_{sd} = -\frac{R_{eq}}{L_{eq}} I_{sd} + \omega I_{sq} - \frac{1}{L_{eq}} V_{bus,d} + \frac{1}{L_{eq}} \sqrt{\frac{3}{2}} V_m \cos(\lambda+\alpha) \\ \dot{I}_{sq} = -\omega I_{sd} - \frac{R_{eq}}{L_{eq}} I_{sq} - \frac{1}{L_{eq}} V_{busq} + \frac{1}{L_{eq}} \sqrt{\frac{3}{2}} V_m \sin(\lambda+\alpha) \\ \dot{V}_{busd} = \frac{1}{C_{eq}} I_{sd} + \omega V_{busq} - \sqrt{\frac{3}{2}} \frac{2\sqrt{3}}{\pi C_{eq}} I_{dc} \\ \dot{V}_{busq} = -\omega V_{busd} + \frac{1}{C_{eq}} I_{sq} \\ \dot{I}_{dc} = \sqrt{\frac{3}{2}} \frac{2\sqrt{3}}{\pi L_F} V_{busd} - \left(\frac{r_\mu}{L_{dc}} + \frac{r_L}{L_{dc}} + \frac{r_c}{L_{dc}} \right) I_{dc} - \frac{1}{L_{dc}} V_{dc} + \frac{r_C \cdot d}{L_{dc}} I_L \\ \dot{V}_{dc} = \frac{1}{C_{dc}} I_{dc} - \frac{d}{C_{dc}} I_L \\ \dot{I}_L = \frac{d}{L} V_{dc} - \frac{1}{L} V_o \\ \dot{V}_o = \frac{1}{C} I_L - \frac{1}{RC} V_o \end{cases} \tag{19}$$

Hitherto, the DQ modeling method is first applied to the power system as shown in Fig. 1 to eliminate the switching action of the three phase rectifier. The equivalent circuits of such power system on DQ frame is depicted in Fig. 7. Then, the GSSA method is used to eliminate the switching behavior of the buck converter. Finally, the time-invariant dynamic model of the power system in Fig. 1 is described in (19). This model can be called the DQ+GSSA model.The DQ+GSSA model given in (19) can be written in the form of (20).

$$\begin{cases} \dot{\mathbf{x}} = \mathbf{A}(\mathbf{x},\mathbf{u})\mathbf{x} + \mathbf{B}(\mathbf{x},\mathbf{u})\mathbf{u} \\ \mathbf{y} = \mathbf{C}(\mathbf{x},\mathbf{u})\mathbf{x} + \mathbf{D}(\mathbf{x},\mathbf{u})\mathbf{u} \end{cases} \tag{20}$$

where state variables:

$$\mathbf{x} = \begin{bmatrix} I_{ds} & I_{qs} & V_{bus,d} & V_{bus,q} & I_{dc} & V_{dc} & I_L & V_o \end{bmatrix}^T$$

input: $\mathbf{u} = \begin{bmatrix} V_m \end{bmatrix}$, output: $\mathbf{y} = \begin{bmatrix} I_{dc} & V_{dc} & I_L & V_o \end{bmatrix}^T$

and the details of **A**, **B**, **C**, and **D** are as follows:

$$\mathbf{A} = \begin{bmatrix} -\frac{R_{eq}}{L_{eq}} & \omega & -\frac{1}{L_{eq}} & 0 & 0 & 0 & 0 & 0 \\ -\omega & -\frac{R_{eq}}{L_{eq}} & 0 & -\frac{1}{L_{eq}} & 0 & 0 & 0 & 0 \\ \frac{1}{C_{eq}} & 0 & 0 & \omega & -\sqrt{\frac{3}{2}}\cdot\frac{2\sqrt{3}}{\pi C_{eq}} & 0 & 0 & 0 \\ 0 & \frac{1}{C_{eq}} & -\omega & 0 & 0 & 0 & 0 & 0 \\ 0 & 0 & \sqrt{\frac{3}{2}}\cdot\frac{2\sqrt{3}}{\pi L_{dc}} & 0 & -\left(\frac{r_\mu + r_L + r_c}{L_{dc}}\right) & -\frac{1}{L_{dc}} & \frac{r_c \cdot d}{L_{dc}} & 0 \\ 0 & 0 & 0 & 0 & \frac{1}{C_{dc}} & 0 & -\frac{d}{C_{dc}} & 0 \\ 0 & 0 & 0 & 0 & 0 & \frac{d}{L} & 0 & -\frac{1}{L} \\ 0 & 0 & 0 & 0 & 0 & 0 & \frac{1}{C} & -\frac{1}{RC} \end{bmatrix}_{8\times 8}$$

$$\mathbf{B} = \begin{bmatrix} \sqrt{\frac{3}{2}}\cdot\frac{\cos(\lambda+\alpha)}{L_{eq}} \\ \sqrt{\frac{3}{2}}\cdot\frac{\sin(\lambda+\alpha)}{L_{eq}} \\ 0 \\ 0 \\ 0 \\ 0 \\ 0 \\ 0 \end{bmatrix}_{8\times 1} \quad \mathbf{C} = \begin{bmatrix} 0 & 0 & 0 & 0 & 1 & 0 & 0 & 0 \\ 0 & 0 & 0 & 0 & 0 & 1 & 0 & 0 \\ 0 & 0 & 0 & 0 & 0 & 0 & 1 & 0 \\ 0 & 0 & 0 & 0 & 0 & 0 & 0 & 1 \end{bmatrix}_{4\times 8} \quad \mathbf{D} = \begin{bmatrix} 0 \\ 0 \\ 0 \\ 0 \end{bmatrix}_{4\times 1}$$

IV. Model Validations

The DQ+GSSA dynamic model in (20) with the details of **A**, **B**, **C**, and **D** is validated by using the simulation in SimPowerSystem™ (SPS™) of SIMULINK via the exact topology model as given in Fig. 8. The set of system parameters for the power system of Fig. 1 is given in Table I.

Fig. 9 shows the I_{dc}, V_{dc}, I_L, and V_o waveforms calculated from the DQ+GSSA model as given in (20) compared with those from the exact topology model to a step change of the voltage source from 200 V_{rms} to 220 V_{rms} that occurs at $t = 0.5$ s. The firing angle of three-phase controlled rectifier and the duty cycle of a buck converter for Fig. 9 are equal to 10 degree and 70%, respectively. Similarly, Fig. 10 – Fig. 14 show the responses for variations in firing angle (10, 20 and 30 degree) and duty cycle (70%, 90%).

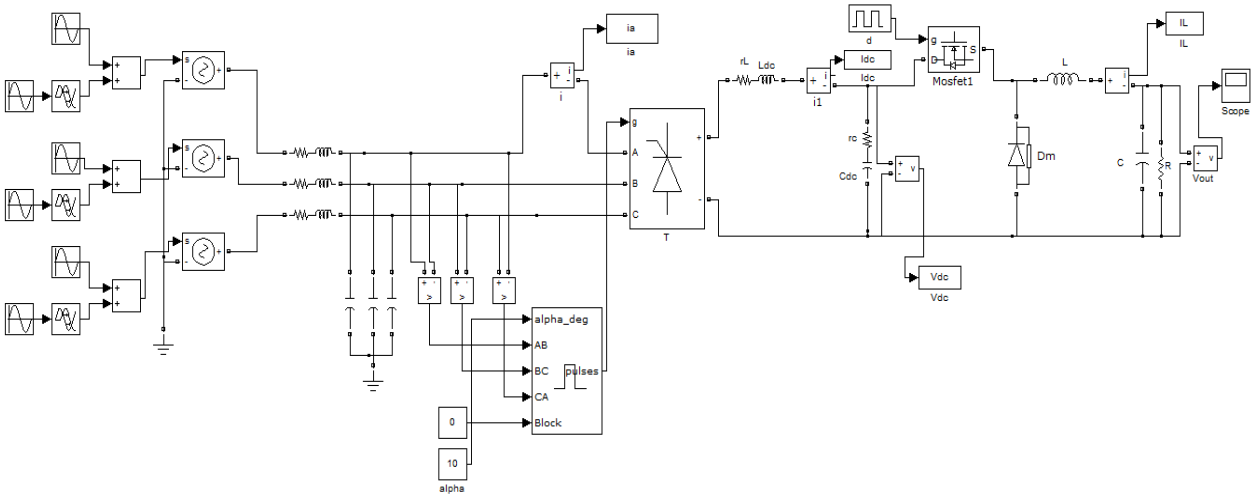

Fig. 8 The exact topology model of the power system in Fig. 1

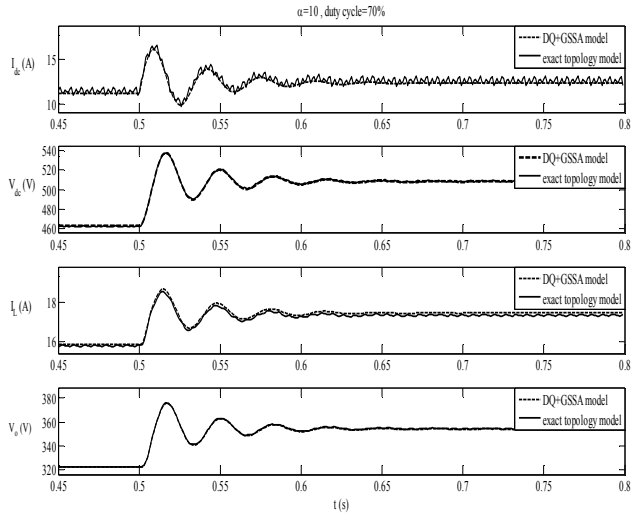

Fig. 9 I_{dc}, V_{dc}, I_L, and V_o responses for α = 10 degree and d = 70%

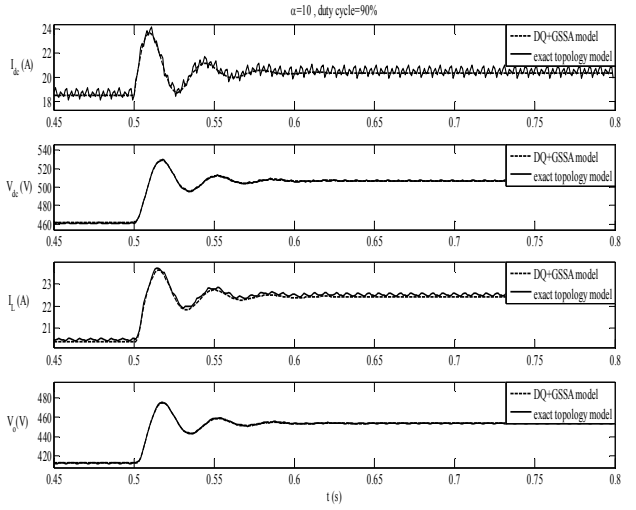

Fig. 10 I_{dc}, V_{dc}, I_L, and V_o responses for α = 10 degree and d = 90%

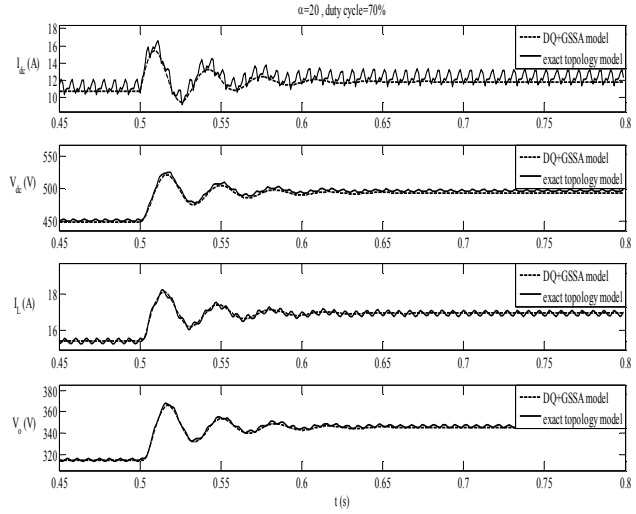

Fig. 11 I_{dc}, V_{dc}, I_L, and V_o responses for α = 20 degree and d = 70%

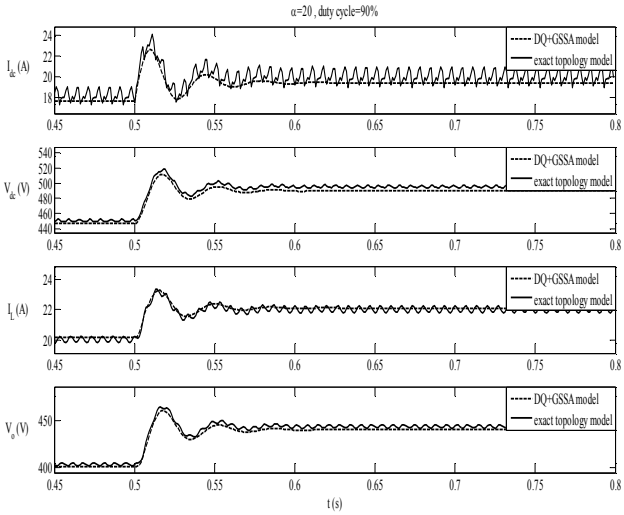

Fig. 12 I_{dc}, V_{dc}, I_L, and V_o responses for α = 20 degree and d = 90%

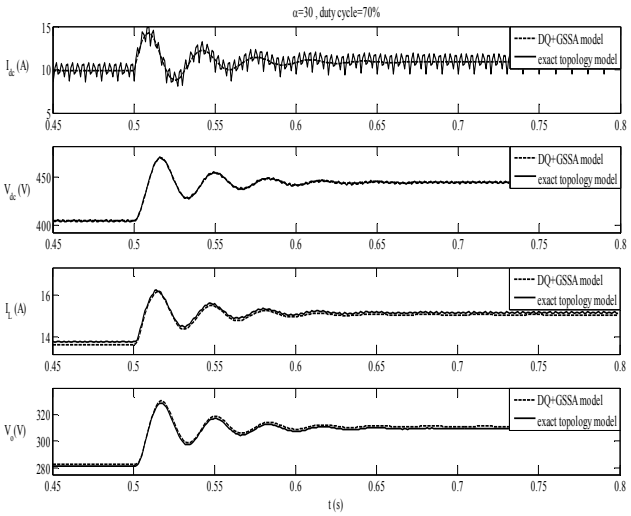

Fig. 13 I_{dc}, V_{dc}, I_L, and V_o responses for α = 30 degree and d = 70%

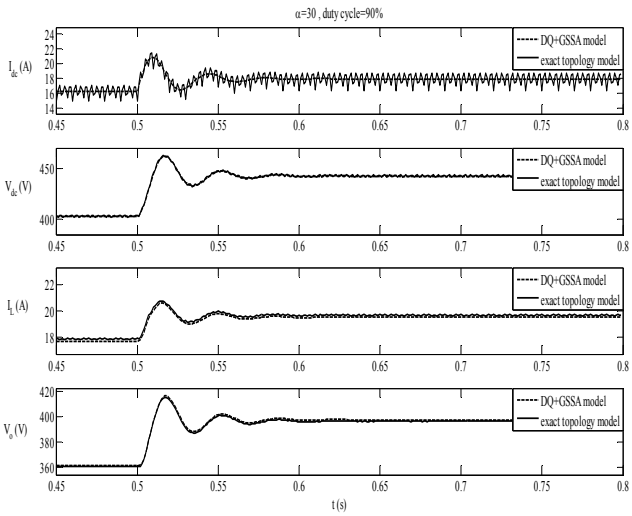

Fig. 14 I_{dc}, V_{dc}, I_L, and V_o responses for α = 30 degree and d = 90%

From the comparison results in Fig. 9 - Fig. 14, an excellent agreement between the proposed model and the exact topology model as given in Fig. 8 is achieved. It confirms that the dynamic model of the system in Fig. 1 derived by the DQ and GSSA methods provides high accuracies in both transient and steady-state responses. The reported model can be used to study the behavior of the whole power system of Fig. 1 and can be used for the system analysis and design. However, it should be noted that the proposed model is valid when the power converters are only operated under the CCM. The current of L_{eq} for CCM operation is depicted in Fig. 15.

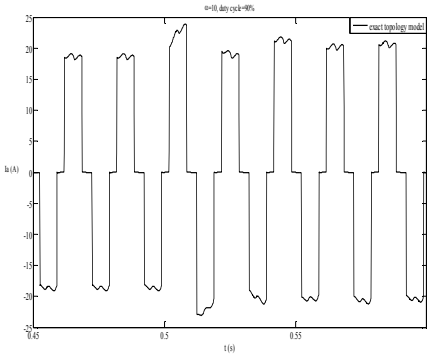

Fig. 15 The inductor current of phase *a* for CCM condition

V. Conclusion

In this paper, the DQ and GSSA modeling methods are presented for modeling a three-phase AC distribution system with a three-phase controlled rectifier, DC-link filters, and uncontrolled buck converter connected to the DC bus. The proposed approach is very useful for modeling the AC distribution system and also concerning a phase shift between source bus and AC bus. Moreover, the resulting converter models can be easily combined with models of other power elements expressed in terms of synchronously rotating frames such as generators, front-end converters, and vector-controlled drives. The simulation results of the exact topology model show that the reported model can provide high accuracies in both transient and steady-state response. The resulting model can then be used for the system analysis and design in the future work.

Acknowledgment

This work was supported by Suranaree University of Technology (SUT) and by the office of the Higher Education Commission under NRU project of Thailand.

References

[1] A. Emadi, 2004. "Modeling and Analysis of Multiconverter DC Power Electronic Systems Using the Generalized State-Space Averaging Method", *IEEE Trans. on Indus. Elect., vol. 51, n. 3*, June, pp. 661-668.

[2] A. Emadi, 2004. "Modeling of Power Electronic Loads in AC Distribution Systems Using the Genearlized State-Space Averaging Method", *IEEE Trans. on Indus. Elect., vol. 51, n. 5*, October, pp. 992-1000.

[3] L. Han, J., Wang, and D., Howe, 2007. "State-space average modelling of 6- and 12-pulse diode rectifiers", *The 12th European Conf. on Power Elect. and Appl.,* Aalborg, Denmark, Sep.

[4] A. Baghramian, and A.J., Forsyth, 2004. "Averaged-Value Models of Twelve-Pulse Rectifiers for Aerospace Applications", *Power Electronics, Machines, and Drives (PEMD 2004)*, University of Edinburgh, UK, March-April, pp.220-225.

[5] S.D. Sudhoff, and O., Wasynczuk, 1993. "Analysis and Average-Value Modeling of Line-Commutated Converter-Synchronous Machine Systems", *IEEE Trans. on Energy Conversion., vol. 8, n. 1*, March, pp. 92-99.

[6] C.T. Rim, D.Y., Hu, and G.H., Cho, 1990. "Transformers as Equivalent Circuits for Switches: General Proofs and D-Q Transformation-Based Analyses", *IEEE Trans. on Indus. Appl., vol. 26, n. 4*, July/August, pp. 777-785.

[7] C.T. Rim, N.S., Choi, G.C., Cho, and G.H., Cho, 1994. "A Complete DC and AC Analysis of Three-Phase Controlled-Current PWM Rectifier Using CircuitD-Q Transformation", *IEEE Trans. on Power Electronics, vol. 9, n. 4*, July, pp. 390-396.

[8] S.B. Han, N.S., Choi, C.T., Rim, and G.H., Cho, 1998. "Modeling and Analysis of Static and Dynamic Characteristics for Buck-Type Three-Phase PWM Rectifier by Circuit DQ Transformation", *IEEE Trans. on Power Electronics*, *vol. 13, n. 2*, March, pp.323-336.

[9] K-N. Areerak, S.V., Bozhko, G.M., Asher, and D.W.P., Thomas, 2008. "Stability Analysis and Modelling of AC-DC System with Mixed Load Using DQ-Transformation Method", *IEEE International Symposium on Industrial Electronics,* Cambridge, UK, 29 June-2 July, pp. 19-24.

[10] K-N. Areerak, S.V., Bozhko, G.M., Asher, and D.W.P., Thomas, 2008. "DQ-Transformation Approach for Modelling and Stability Analysis of AC-DC Power System with Controlled PWM Rectifier and Constant Power Loads", *13th International Power Electronics and Motion Control Conference (EPE-PEMC 2008),* Poznan, Poland, 1-3 September.

[11] K-N. Areerak, S., Bozhko, G., Asher, L.de, Lillo, A., Watson, T., Wu, and D.W.P., Thomas, 2009. "The Stability Analysis of AC-DC Systems including Actuator Dynamics for Aircraft Power Systems", *13th European Conference on Power Electronics and Applications (EPE 2009)*, Barcelona, Spain, 8-10 September.

[12] K. Chaijarurnudomrung, K-N., Areerak, and K-L., Areerak, 2010. "Modeling of Three-phase Controlled Rectifier using a DQ method", *2010 International Conference on Advances in Energy Engineering (ICAEE 2010)*, Beijing, China: June 19-20, pp.56-59.

[13] N. Mohan, T.M. Underland, and W.P. Robbins, *Power Electronics: Converters, Applications, and Design,* John Wiley & Son, USA, 2003.

[14] C-M Ong, "Dynamic Simulation of Electric Machinery using MATLAB/Simulink," Prentice Hall, 1998.

P. Ruttanee received the B.S. degree in electrical engineering from Suranaree University of Technology (SUT), Nakhon Ratchasima, Thailand, in 2010, where he is currently studying toward the M.Eng. degree in electrical engineering. His main research interests include stability analysis, modeling of power electronic system, digital control, FPGA, and AI applications.

K-N. Areerak received the B.Eng. and M.Eng. degrees from Suranaree University of Technology (SUT), Nakhon Ratchasima, Thailand, in 2000 and 2001, respectively and the Ph.D. degree from the University of Nottingham, Nottingham, UK., in 2009, all in electrical engineering. In 2002, he was a Lecturer in the Electrical and Electronic Department, Rangsit University, Thailand. Since 2003, he has been a Lecturer in the School of Electrical Engineering, SUT. His main research interests include system identifications, artificial intelligence application, stability analysis of power systems with constant power loads, modeling and control of power electronic based systems, and control theory.

K-L. Areerak received the B.Eng, M.Eng, and Ph.D. degrees in electrical engineering from Suranaree University of Technology (SUT), Thailand, in 2000, 2003, and 2007, respectively. Since 2007, he has been a Lecturer and Head of Power Quality Research Unit (PQRU) in the School of Electrical Engineering, SUT. He received the Assistant Professor in Electrical Engineering in 2009. His main research interests include active power filter, harmonic elimination, AI application, motor drive, and intelligence control system.